1521-0103/381/3/236–246$35.00
THE JOURNAL OF PHARMACOLOGY AND EXPERIMENTAL THERAPEUTICS

dx.doi.org/10.1124/jpet.121.000907
J Pharmacol Exp Ther 381:236–246, June 2022

Angiotensin-Converting Enzyme 2 Inhibits Lipopolysaccharide-Caused Lung Fibrosis via Downregulating the Transforming Growth Factor β-1/Smad2/Smad3 Pathway

Xingsheng Lin, Wenhao Lin, Yingfeng Zhuang, and Fengying Gao

Department of Intensive Care Unit, Shengli Clinical Medical College of Fujian Medical University, Fujian Provincial Hospital, Fujian, China (X.L., Y.Z.); Department of Clinical Medicine, Shengli Clinical Medical College, Fujian Medical University, Fujian, China (W.L.); and Department of Respiratory Medicine, Shanghai Construction Group Hospital, Shanghai, China (F.G.)

Received September 5, 2021; accepted March 4, 2022

ABSTRACT

Background: In our previous studies, angiotensin-converting enzyme 2 (ACE2) was shown to alleviate the severity of acute lung injury, but its effects on the development of lung injury–caused lung fibrosis have not been studied. Methods: In the present study, the effects of ACE2 on lipopolysaccharide (LPS)-induced fibrosis in the lung were studied. The role of epithelial-mesenchymal transition (EMT) and that of the transforming growth factor β-1 (TGF-β1)/Smad2/Smad3 pathway in LPS-induced fibrosis in the lung were investigated. Results: ACE2 expression in the mouse model of LPS-induced lung fibrosis was significantly increased. ACE2 activator diminazene aceturate (DIZE) significantly reduced pulmonary fibrosis, decreased alpha-smooth muscle actin expression, collagen I, hydroxyproline, and TGF-β1 in the lung. DIZE significantly decreased TGF-β1 expression and the activation of Smad2 and Smad3. ACE2 overexpression inhibited the LPS-induced EMT in MLE-12 cells (lung epithelial cells) and small interfering RNA treatment of ACE2 stimulated EMT. ACE2 overexpression also inhibited TGF-β1 expression and activation of Smad2 and Smad3 in MLE-12 cells. Finally, after MLE-12 cells were treated with both ACE2 and TGF-β1 plasmid, TGF-β1 plasmid significantly abolished the effect of ACE2 plasmid on the EMT in MLE-12 cells. Conclusion: Combined with the in vivo study, it was revealed that ACE2 can suppress the TGF-β1/Smad2/Smad3 pathway in lung type II epithelial cells, thus reversing their EMT and lung fibrosis. The present study provides basic research data for the application of ACE2 in lung injury–caused lung fibrosis treatment and clarifies the intervention mechanism of ACE2 in pulmonary fibrosis, which has potential value for clinical application.

SIGNIFICANCE STATEMENT

Angiotensin-converting enzyme 2 (ACE2) can inhibit the epithelial-mesenchymal transition (EMT) in lung type II epithelial cells and lung fibrosis. ACE2 can regulate the transforming growth factor β-1/Smad2/Smad3 pathway in lung type II epithelial cells, which may be the underlying mechanism of ACE2's effect on EMT and lung fibrosis.

Introduction

Acute lung injury (ALI) is secondary diffuse lung parenchyma of the inflammation cascade involving a variety of inflammatory media and effector cells, which share the same pathophysiological changes (Wang et al., 2014). They are common clinical respiratory diseases with complex etiology and pathogenesis and high mortality rates (Butt et al., 2016). Acute respiratory distress syndrome (ARDS) in the later stage can cause interstitial fibrosis and bronchofibrosis and can even form honeycomb lung due to the progress of pulmonary interstitial fibrosis and extensive destruction of lung parenchyma, which leads to serious and irreversible damage to lung function (Antunes et al., 2014). In addition, after the novel severe acute respiratory syndrome (SARS) coronavirus 2 broke out around the world, there have been reports regarding the post–coronavirus disease 2019 (COVID-19) pneumonia pulmonary fibrosis (Shi et al., 2020; Tale et al., 2020). Even though there is still some debate on whether survivors of COVID-19 will fully recover or have progressive fibrosis after the COVID-19 infection (McDonald, 2021), previous data from previous coronavirus infections such as the SARS outbreak in 2003 and Middle East respiratory syndrome and the subsequent ALI/ARDS indicated there could be substantial fibrotic consequences following SARS coronavirus 2 infection (George et al., 2020). Therefore, exploring the mechanism of lung fibrosis could potentially provide new molecule targets for the treatment of lung fibrosis occurring in the COVID-19 pandemic.

Transforming growth factor β-1 (TGF-β1) is an extracellular matrix (ECM) deposition promoter, which can increase synthesis of the ECM and reduce degradation by upregulating the transcription and translation of matrix component genes, thus

This work was supported by Fujian Provincial Natural Science Foundation of China [Grant 2018J01261].
The authors declare no competing interests.
dx.doi.org/10.1124/jpet.121.000907.

ABBREVIATIONS: ACE2, angiotensin-converting enzyme 2; ALI, acute lung injury; Ang, angiotensin; ARDS, acute respiratory distress syndrome; BALF, bronchoalveolar lavage fluid; COVID-19, coronavirus disease 2019; DIZE, diminazene aceturate; ECM, extracellular matrix; EMT, epithelial-mesenchymal transition; LPS, lipopolysaccharide; MasR, Mas receptor; SARS, severe acute respiratory syndrome; siRNA, small interfering RNA; α-SMA, alpha-smooth muscle actin; TGF-β1, transforming growth factor β-1.

causing fibrosis (Liu, 2006). TGF-β1 expression in normal lung tissue is very low but can be stimulated by endotoxins and participates in increasing the permeability of pulmonary capillaries and the transition from lung injury to early pulmonary fibrosis (Mackinnon et al., 2012). Smad proteins are the main signal transduction molecules of TGF-β1 (Attisano and Wrana, 2002). TGF-β1 was confirmed to increase the permeability of endothelial cells by phosphorylation of Smad2, and Smad2 small interfering RNA (siRNA) reversed the effects of TGF-β1 on endothelial cell permeability, indicating Smad2 plays a leading role in how TGF-β1 affects endothelial cell permeability (Lu et al., 2006). TGF-β1 can mediate the proliferation of pulmonary fibroblasts and production of the ECM, which contributes to pulmonary fibrosis in the later stage (Lu et al., 2006). Smads are a family of cytoplasmic signal transduction proteins regulated by TGF-β1 and are divided into receptor-regulated Smads (such as Smad2/3), universal Smads, and inhibitory Smads (Wu et al., 2012).

The classic renin-angiotensin system members include renin, angiotensinogen, and angiotensin-converting enzyme (White et al., 2015). Improper activation of the renin-angiotensin system produces excessive angiotensin (Ang) II and causes cell injury (Kobori et al., 2007). In the in vitro studies, Ang II could significantly aggravate the inflammatory damage of lipopolysaccharide (LPS) on pulmonary microvascular permeability in rats by mediating Ang II 1 receptor (Zhang and Sun, 2005). Angiotensin-converting enzyme 2 (ACE2) is an angiotensin-converting enzyme homologous compound, which hydrolyzes Ang II to Ang1-7 (Li et al., 2012). Ang1-7 plays a protective role in the body through its main receptor, Mas receptor (MasR) (Santos et al., 2003). It can antagonize most effects of Ang II, such as inducing vasodilation, increasing organ perfusion, and improving myocardial remodeling as well as preventing renal fibrosis and lung tumor proliferation (Simko et al., 2021). In our previous studies, ACE2 exhibits the ability to alleviate ALI symptoms (Fang et al., 2019; Huang et al., 2020). Diminazene aceturate (DIZE) is a widely used drug against *Trypanosoma* and was recently shown to be an ACE2 agonist (Tao et al., 2016). Recently, in animal models of pulmonary hypertension and myocardial infarction, DIZE was shown to activate ACE2, promote Ang II degradation to Ang 1-7, and play a protective role (Qaradakhi et al., 2020). In our previous experiments, DIZE treatment was confirmed to increase ACE2 protein expression in the lung and effectively reduce lung injury in animals (Fang et al., 2019). Hence, whether activation of ACE2 can inhibit lung injury–related fibrosis and the mechanism requires further study.

As the effects and mechanism of the ACE2/Ang1-7/Mas axis in the development of LPS-caused lung fibrosis have not yet been investigated, the effects of ACE2 on LPS-caused lung fibrosis were evaluated in the study. The epithelial–mesenchymal transition (EMT) is associated with embryonic development, inflammation, wound healing, tumor progression, and organ fibrosis (Puisieux et al., 2014). Whether the EMT is involved in LPS-caused lung fibrosis is unknown; thus, the contribution of the EMT to LPS-caused lung fibrosis and the mechanism of ACE2 on lung fibrosis were investigated.

Materials and Methods

Animals and Groups. C57BL/6 mice (male, 6–8 weeks, 20–25 g) were purchased from the animal center of Fujian Medical University and housed with freely accessed water/food and 12-hour light/12-hour dark cycles. In part I, mice were randomly grouped into two groups, control and model (n = 12). After mice were injected with ketamine (100 mg/kg i.p.) and acepromazine (5.0 mg/kg i.p.), mice in the control group received a single intratracheal injection of phosphate-buffered saline (PBS; 30 μL). Mice in the model group were treated with intratracheal administration of LPS in PBS (5.0 mg/kg, Sigma-Aldrich) diffused in 30 μL of PBS. In part II, mice were randomly grouped into the following groups: control, model+vehicle, model+DIZE-10 mg/kg, model+DIZE-20 mg/kg, and model+DIZE-40 mg/kg (n = 12). After mice were injected with ketamine/acepromazine, mice in the model+vehicle group received intratracheal administration of LPS and were continuously infused with saline. Mice in the model+DIZE-10 mg/kg, model+DIZE-20 mg/kg, and model+DIZE-40 mg/kg groups received intratracheal administration of LPS and were continuously infused with DIZE (10–40 mg/kg per day). The whole study was approved by Fujian Medical University. Approval for all experimental protocols was granted by the Animal Care Committee of Fujian Medical University.

LPS-Caused Lung Fibrosis and DIZE Treatment. Similar to Li et al. (2018), male C57BL/6 mice received a single intratracheal administration of LPS (5.0 mg/kg, Sigma-Aldrich) diffused in 30 μL of PBS. After mice were injected with ketamine/acepromazine, they received orotracheal intubation with a 20-G intravenous cannula. The same volume of PBS was injected as control. Mice were treated with the ACE2 activator DIZE as previously described (Fang et al., 2019). Briefly, mice received daily intraperitoneal injections of DIZE (10, 20, or 40 mg/kg, Santa Cruz) for 7 days after LPS administration.

Specimen Collection. At day 28 after LPS injection, mice were injected with ketamine/acepromazine and euthanized by quick dislocation of cervical vertebra. The bronchoalveolar lavage fluid (BALF) was collected. After the trachea was exposed, it was cannulated with 20-G cannulas and lavaged with PBS (containing 2 mM ethylene diamine tetraacetic acid) three times to collect BALF. Next, the left lower lobe of lung was collected and kept in 10% formaldehyde for the following experiments; the right lung tissue (150 mg) was kept at −80°C for further examination.

Pathologic Examination of Lung Tissue. The left lower lobe of lung was cut into sections and stained with H&E method. The following pathologic changes were recorded under a light microscope: alveolar edema, inflammatory cell infiltration, alveolar hemorrhage and microthrombosis, fibroblast infiltration, and type II alveolar epithelial cell proliferation.

Masson staining was performed in paraffin sections and then washed with water. The mixture of ferro hematoxylin A and B was added to the tissue at a ratio of 1:1 for 3 minutes, treated with 1% hydrochloric acid for 5 seconds, and washed with water. Next, the slices were placed in Ponceau dye for 7 minutes and cleaned with water. They were treated with molybdophosphoric acid for 3 minutes and stained with aniline blue for 5 minutes. Finally, slices were treated with glacial acetic acid for 1 minute followed by dehydration (95% alcohol for 3 minutes, 95% alcohol again for 3 minutes, anhydrous ethanol for 5 minutes, anhydrous ethanol again for 5 minutes, xylene for 5 minutes, and xylene again for 5 minutes) and sealed with neutral gum.

The level of alpha-smooth muscle actin (α-SMA) was detected using immunohistochemistry based on the method of Wan et al. (2019). The lung tissue was deparaffinized, incubated with 1% albumin solution, blocked with goat serum, then incubated with rabbit anti–α-SMA primary antibody (1:2000, Sigma) and goat anti-rabbit IgG secondary antibody (1:1000, Sigma).

Measurement of Collagen I in Lung Tissue. After the lung tissues were weighed, the prepared lysis solution (mass: volume ratio 1:50) was added in proportion. After, the tissues were homogenized using an ultrasonic processor and centrifuged for 10 minutes (12 000 ×g,

4°C). The supernatant was then gathered and added to 96-well plates. After diluting the standard solution, 100 μL was added to the 96-well plates, which were transferred to 37°C for 60 minutes. One hundred microliters of working liquid of test solution was added. The microplates were tightly sealed with film and kept at 37°C (60 minutes). The microplates were rinsed with prepared washing solution, and 100 μL of the working liquid test solution B was added into each well. The microplates were then kept at 37°C (30 minutes). The liquid was discarded again, the microplates washed with washing solution, and 90 μL of 3,3′,5,5′-Tetramethylbenzidine solution was added. The microplates were placed at 37°C in the dark for 10 minutes. Next, 50 μL of stop reaction solution was mixed. The preheated enzyme standard instrument was used for reading at 450 nm. The light density of each well was detected and the values saved for analysis.

Determination of Hydroxyproline in Lung Tissue. A lung tissue sample (50 mg) was put in a clean microfuge tube. Next, 1 mL of hydrolysate was added to each tube. The tubes were covered, tightly sealed, and placed in boiling water for 20 minutes. Then, 30 mg of activated carbon was added to 3 mL of diluted hydrolysate and mixed well. The tubes were centrifuged for 5 minutes at 3500 ×g and 1 mL of supernatant removed for analysis. Next, 0.5 mL reagent was mixed in each sample tube and placed for 10 minutes at 25°C. Then, 20.5 mL of reagent was added and kept for 5 minutes, then kept with 30.5 mL of reagent addition for 5 minutes. The microfuge tube was sealed with film, incubated in a 60°C water bath for 15 minutes, cooled naturally, centrifuged for 5 minutes at 3500 ×g, and 100 μL supernatant was carefully removed. A one-hundred-microliter sample from each group was added to 96-well plates, and 550 nm wavelength was used for analysis. The optical density value of each well was measured and the data recorded and saved for analysis.

Determination of TGF-β1 in BALF Using ELISA. The standard was diluted, the sample activation reagent prepared, and 100 μL of mice alveolar lavage solution was taken from each group. Next, 20 μL of activation reagent A was added. After 10 minutes, 20 μL of activating reagent B solution was added and placed at 37°C for 90 minutes. Then, the liquid was discarded and 100 μL of prepared biotin-labeled anti-mouse TGF-β1 antibody was added. The plates were incubated at 37°C for 60 minutes. The liquid was discarded; the plates were washed five times with washing liquid. The working solution of avidin peroxidase complex was prepared in advance and placed at 37°C for 30 minutes. The liquid was discarded; the plates were washed five times with washing solution, and 90 μL of TMB substrate was added. The plates were sealed, placed in at 37°C in the dark for 15 minutes, and 50 μL stop reaction solution was added. The enzyme

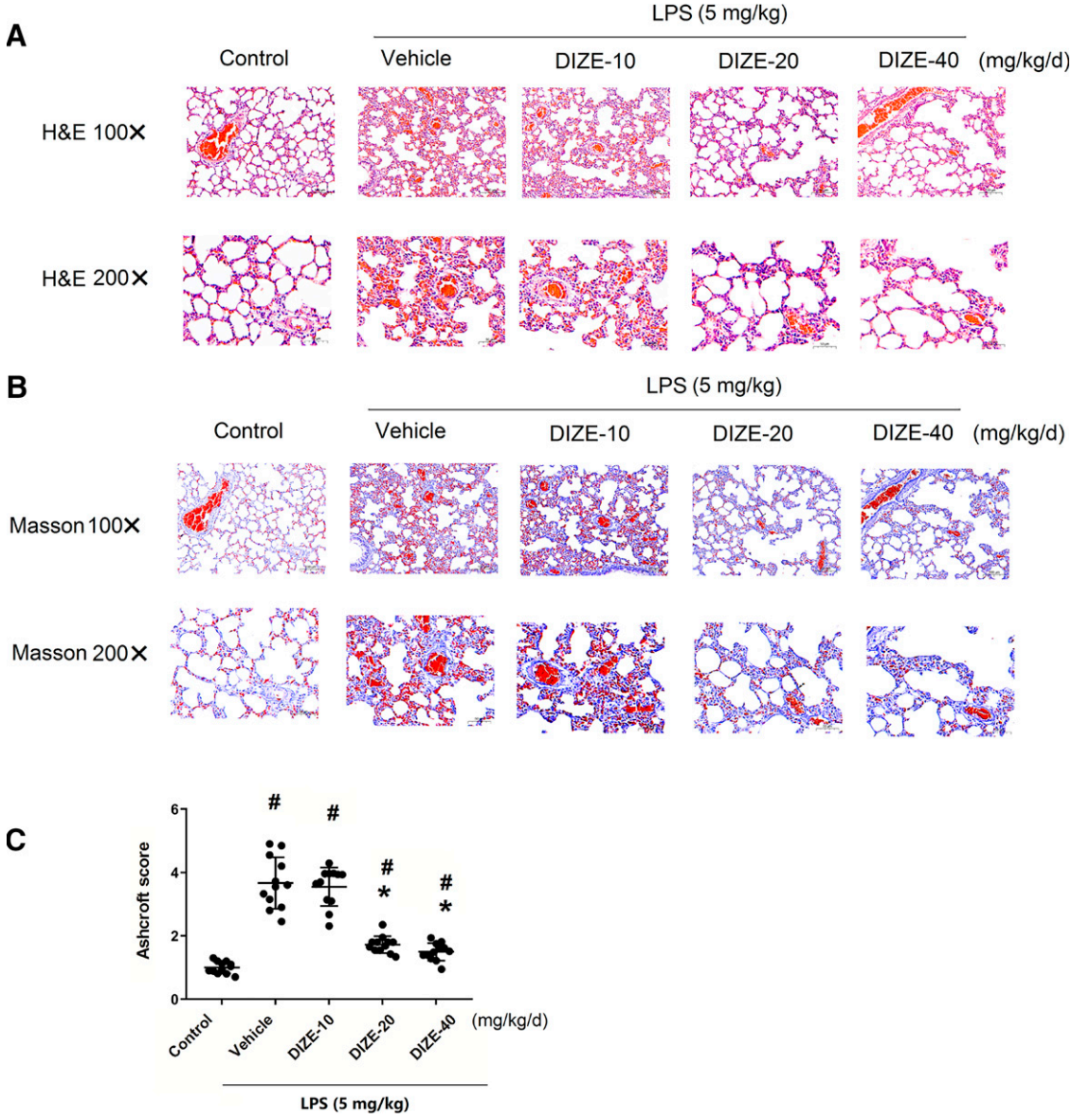

Fig. 1. The effects of DIZE on LPS-induced histologic and fibrosis changes. (A) The lung histologic changes demonstrated by H&E staining. The dosage of LPS was 5.0 mg/kg. (B) The lung fibrosis demonstrated by Masson staining. (C) The results of Ashcroft scores. #, $P < 0.05$ compared with control; *, $P < 0.05$ compared with the LPS+vehicle group. $N = 12$.

standard was immediately used at 450 nm for the detection of light density in each well. The values for each group were recorded, and the concentration of TGF-β1 was calculated.

Quantitative Polymerase Chain Reaction. The procedure was previously described by Shu et al. (2015). Briefly, firstly, the RNA was separated from the lung tissue with an RNA extraction kit (Promega). The primers used were the following: ACE2, forward: 5′-CACCATGT-CAAGCTCTTCCT-3′, reverse: 5′-AAAGGAGGTCTGAACATCATCAG-3′; TGF-β1, forward: 5′-GACTCTCCACCTGCAAGACCAT-3′, reverse: 5′-GGGACTGGCGAGCCTTAGTT-3′; Smad2, forward: AAGCCATCAC-CACTCAGAATTG, reverse: CACTGATCTACCGTATTTGCTGT; Smad3, forward: 5′-GAGTAGAGACGCCAGTTCTACC-3′, reverse: 5′-GGTTTG-GAGAACCTGCGTCCAT-3′; and glyceraldehyde-3-phosphate dehydrogenase, forward: AGGAGTAAGAAACCCTGGAC, reverse: CTGGGATG-GAATTGTGAG. The polymerase chain reaction conditions were set as 95°C for 10 minutes; 95°C for 15 seconds, 40 cycles; and 60°C for 60 seconds. The $2^{-\Delta\Delta Ct}$ method was adopted to measure the mRNA content.

Transfections and siRNA Interference. Cells were transfected with plasmid DNA carrying the transcriptional target sequence of ACE2 promoter according to Zhang et al. (2018). The cells were also transfected with empty plasmid to establish a plasmid control. For ACE2 siRNA, cells were treated with Lipofectamine 3000 (Invitrogen, Carlsbad, CA) following the instruction. The following primers were used for ACE2 siRNA: forward, 5′-GAGGAGACUAUGAAGUAAATT-3′ and reverse, 5′-UUUACUUCAUAGUCUCCUCTT-3′.

Western Blot. As previously described (Zhang et al., 2019), the expression of ACE2, TGF-β1, phosphorylated Smad2 (p-Smad2), Smad2, p-Smad3, Smad3, E-cadherin, α-SMA, vimentin, or glyceraldehyde-3-phosphate dehydrogenase (Sigma-Aldrich) were examined by western blot.

Statistical Analyses. All the data are shown as mean ± S.D.. The statistical analyses were performed with one-way ANOVA followed by Newman–Keuls test. $P < 0.05$ was considered statistically significant.

Results

ACE2 Activator DIZE Attenuates LPS-Caused Lung Fibrosis. After mice were treated with LPS (5 mg/kg) and different dosages of ACE2 activator DIZE (10–40 mg/kg per day), the degree of pulmonary fibrosis was measured using H&E staining, Masson staining, and Ashcroft scores. As shown in Fig. 1A, in the model+vehicle and model+DIZE-10 mg/kg groups, the alveoli structure was destroyed, the alveoli cavity was reduced, and exfoliated alveolar epithelium and protein exudates were present in the cavity. Areas with obvious collagen deposition and fibrosis were observed. Collagen fibers proliferated in strips, forming diffuse pulmonary fibrosis. In the model+DIZE-20 mg/kg and model+DIZE-40 mg/kg groups,

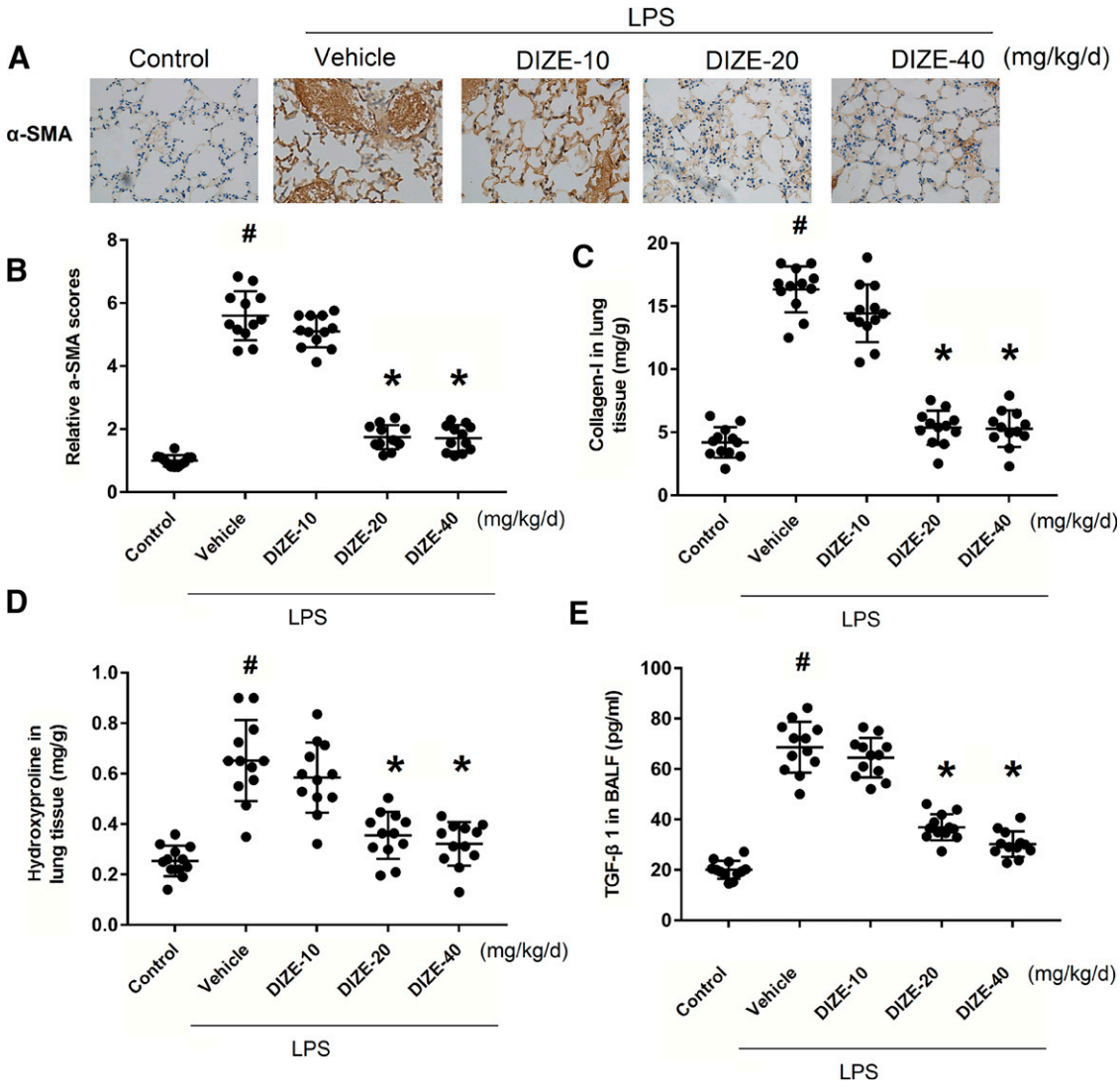

Fig. 2. The effects of DIZE on LPS-induced changes on fibrosis related biomarkers. (A) The expression of α-SMA in the lung measured by immunohistochemistry. (B) The results of α-SMA scores calculated from immunohistochemistry. (C and D) The levels of collagen I and hydroxyproline in lung tissue. (E) The levels of TGF-β1 in BALF. #, $P < 0.05$ compared with control; *, $P < 0.05$ compared with the LPS+vehicle group. $N = 12$.

fibroblasts exhibit slight proliferation, collagen fibers were deposited in the pleura and alveolar septum, and changes of mild and moderate pulmonary fibrosis occurred; the scope of the lesions was limited. As shown in Fig. 1B, in the model+vehicle and model+DIZE-10 mg/kg groups, the alveoli structure was destroyed and fascicular or large collagenous fibers were deposited in the lung interstitium (blue), forming typical fibrosis changes. In the model+DIZE-20 mg/kg and model+DIZE-40 mg/kg groups, the alveolar space was widened, and blue collagen fibers were found in the alveolar septum and lung interstitial space; however, the color was lighter than in the model+vehicle group, and the collagen fibers were significantly reduced. Fig. 1C shows the Ashcroft scores. The Ashcroft scores in the model+vehicle and model+DIZE-10 mg/kg groups were increased compared with control ($P < 0.05$, $n = 12$). The Ashcroft scores in the model+DIZE-20 mg/kg and model+DIZE-40 mg/kg groups were significantly decreased in the model+vehicle group ($P < 0.05$, $n = 12$).

Effects of DIZE on α-SMA Expression and Collagen I, Hydroxyproline, and TGF-β1 in the Lung. Fig. 2A shows the α-SMA expression measured with immunohistochemistry method. Fig. 2B shows the α-SMA expression scores. The level of α-SMA was significantly raised in the model+vehicle and model+DIZE-10 mg/kg groups compared with control ($P < 0.05$, $n = 12$) but was decreased by 20 mg/kg and 40 mg/kg DIZE treatments ($P < 0.05$ compared with control, $n = 12$). Fig. 2, C and D show the collagen I and hydroxyproline concentrations in lung tissue, which were significantly raised in the model+vehicle and model+DIZE-10 mg/kg groups compared with control ($P < 0.05$, $n = 12$). In the model+DIZE-20 mg/kg and model+DIZE-40 mg/kg groups, collagen I and hydroxyproline concentrations in lung tissue were significantly decreased ($P < 0.05$ compared with control, $n = 12$). Fig. 2E shows TGF-β1 in BALF was significantly increased in the model+vehicle and model+DIZE-10 mg/kg groups ($P < 0.05$ compared with control, $n = 12$) but decreased in the model+DIZE-20 mg/kg and model+DIZE-40 mg/kg groups ($P < 0.05$ compared with model+vehicle group, $n = 12$).

The Expression of ACE2, TGF-β1, and Smad2/3 in the Mouse Model of LPS-Induced Lung Fibrosis. Firstly, the mRNA levels of ACE2, TGF-β1, and Smad2/3 in the lung tissue were measured. The results are shown in Fig. 3, A–D. Compared with control, the ACE2 mRNA level was significantly decreased in the model group ($P < 0.05$, $n = 12$). By contrast, the TGF-β1 mRNA level was significantly increased in the model group ($P < 0.05$, $n = 12$). However, the Smad2 and Smad3 mRNA levels were not dramatically changed in the model group ($P > 0.05$, $n = 12$). Secondly, protein levels of ACE2, TGF-β1, p-Smad2, p-Smad3, Smad2, and Smad3 were measured in the lung tissue of mice (Fig. 3, E–G). ACE2 protein expression was dramatically decreased in the model group, and TGF-β1 protein expression was dramatically increased ($P < 0.05$, $n = 12$). The p-Smad2/Smad2 and p-Smad3/Smad3 ratios were adequately increased in the model group ($P < 0.05$, $n = 12$), indicating activation of the TGF-β1/Smad2/Smad3 pathway following LPS stress in vivo.

Effects of DIZE on the Level of TGF-β1 and Smad2/3 in Mice. To measure the effects of ACE2 on the TGF-β1/Smad2/3 pathway, mice were treated with DIZE, and the mRNA and protein expression of TGF-β1 and Smad2/3 in the lung was measured. The TGF-β1 mRNA levels were adequately decreased by 20 mg/kg and 40 mg/kg DIZE treatments (Fig. 4A), whereas Smad2 and Smad3 mRNA levels were not significantly changed between groups (Fig. 4, B and C). Fig. 4D shows the western blot results of ACE2, TGF-β1, p-Smad2/3, and Smad2/3 expression in the lung tissue; 20 mg/kg and 40 mg/kg DIZE treatments significantly decreased the expression of TGF-β1 and p-Smad2/3 but did not affect Smad2 and Smad3 expression, indicating DIZE inhibited the activation of TGF-β1/Smad2/Smad3 pathway in vivo.

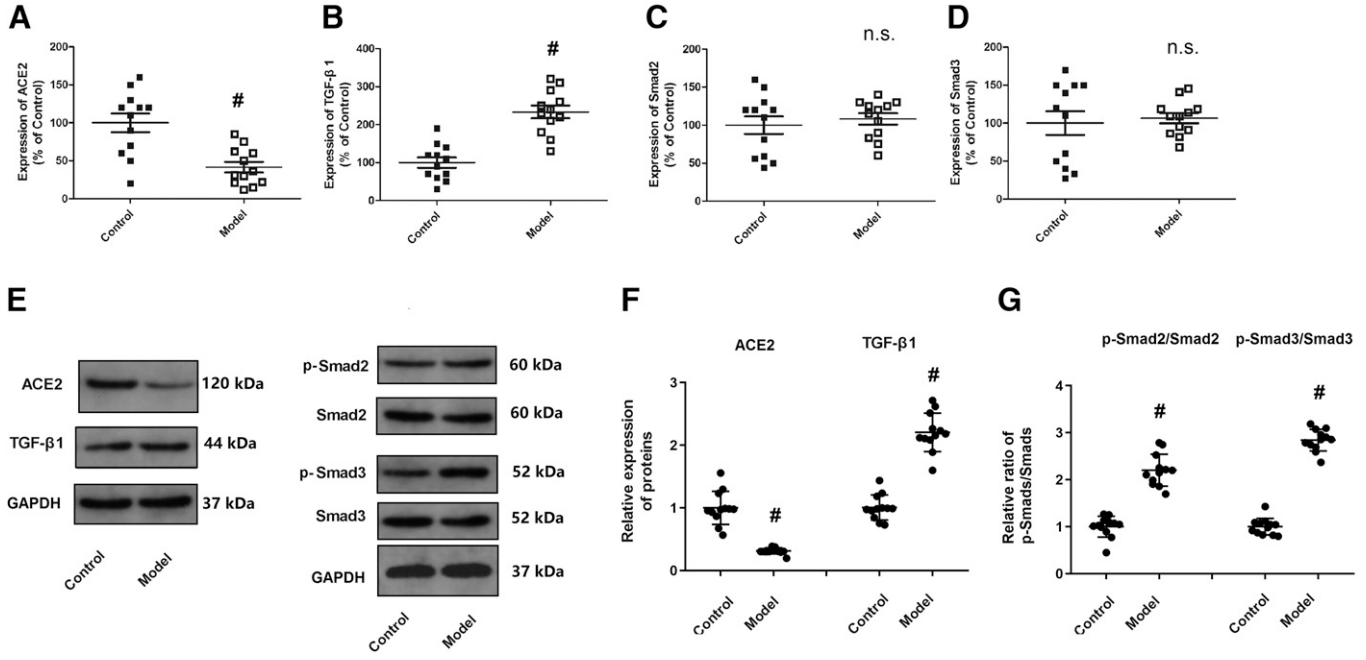

Fig. 3. The mRNA and protein expression of ACE2, TGF-β1, Smad2, and Smad3 in the mouse model of LPS-induced lung fibrosis. (A–D) The mRNA levels of ACE2, TGF-β1, Smad2, and Smad3 in control mice and model mice. (E) The representative images of western blot; (F) shows the relative changes of ACE2 and TGF-β1; (G) shows the relative ratios of p-Smad2/Smad2 andp-Smad3/Smad3. #, $P < 0.05$ compared with control. $N = 12$.

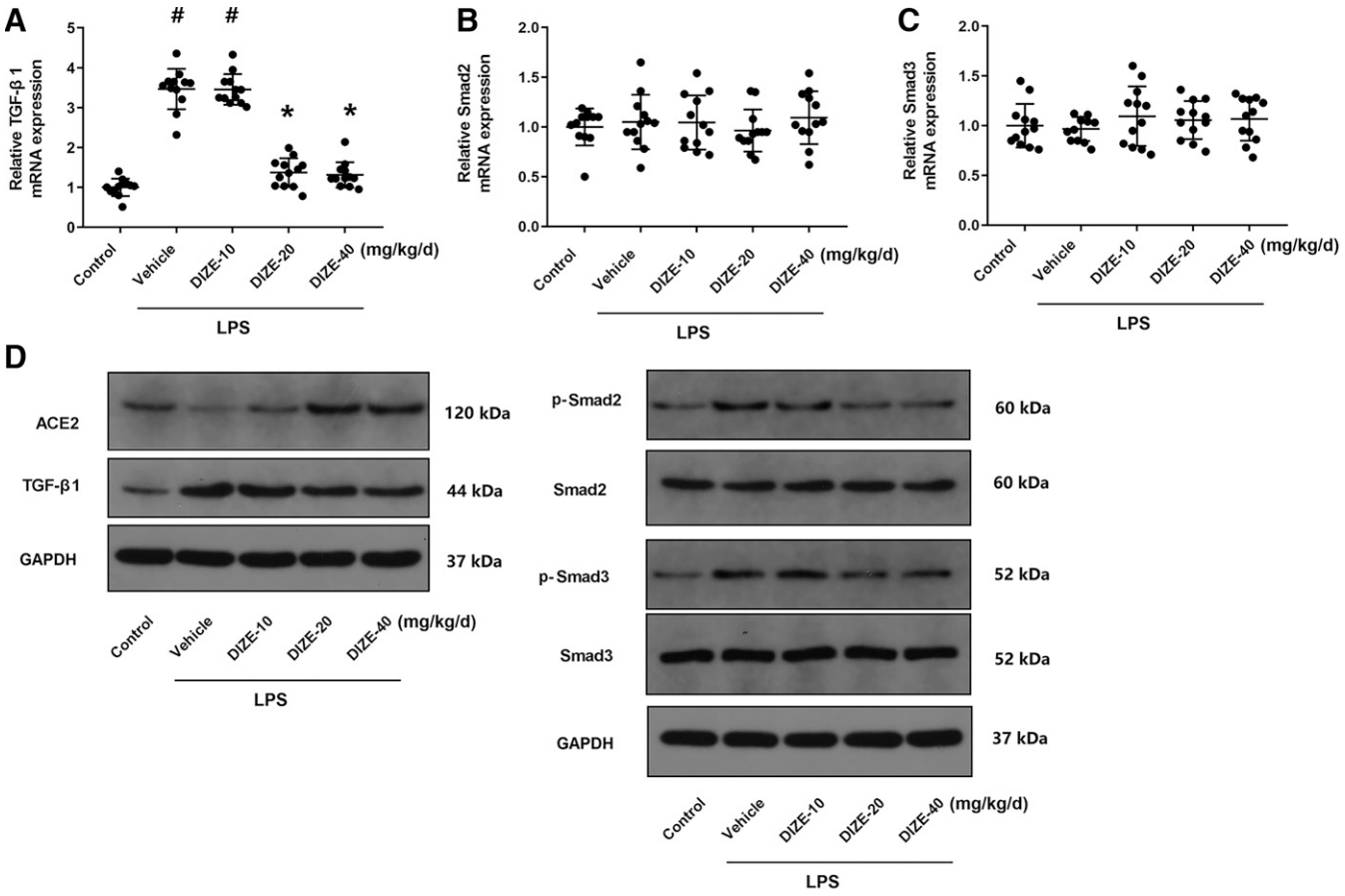

Fig. 4. The effects of DIZE on mRNA and protein expression of TGF-β1, Smad2, and Smad3 in mice lung. After mice were treated with LPS and DIZE, the mRNA and protein expression of TGF-β1, Smad2 and Smad3 in mice lungs were measured. (A–C) The mRNA levels of TGF-β1, Smad2, and Smad3 in control mice and model mice. (D) The representative images of western blot. $^{\#}$, $P < 0.05$ compared with control; *, $P < 0.05$ compared with the LPS+vehicle group. $N = 12$.

Effects of ACE2 Overexpression or siRNA on the EMT in MLE-12 Cells. To examine the antifibrosis effects of ACE2 on lung, the type II epithelial cell line MLE-12 cells were treated with LPS and ACE2 plasmid or ACE2 siRNA. Then, the expression of E-cadherin, α-SMA, and vimentin was determined. Fig. 5A shows that the expression of ACE2 was significantly increased in the ACE2 plasmid group but significantly decreased in the ACE2 siRNA group, indicating that the ACE2 plasmid or ACE2 siRNA was successful. Fig. 5, B–D show the protein expression of E-cadherin, α-SMA, and vimentin. The E-cadherin protein expression level was dramatically reduced in the model group, increased by ACE2 plasmid, and reduced by ACE2 siRNA. By contrast, the expression of α-SMA and vimentin were significantly escalated in the model group, decreased by ACE2 plasmid, and increased by ACE2 siRNA. These results suggested that ACE2 inhibited the EMT in MLE-12 cells.

Effects of ACE2 Overexpression or siRNA on the Levels of TGF-β1 and Smad2/3 in MLE-12 Cells. To examine the effects of ACE2 on the TGF-β1/Smad2/Smad3 pathway, MLE-12 cells were treated with ACE2 plasmid or ACE2 siRNA, and the mRNA and protein expression of TGF-β1 and Smad2/3 in the lung were measured. As shown in Fig. 6A, the TGF-β1 mRNA level was decreased by ACE2 plasmid but increased by ACE2 siRNA. As shown in Fig. 6, B and C, the mRNA levels of Smad2 and Smad3 were not significantly changed between groups. Fig. 6D shows TGF-β1, p-Smad2, p-Smad3, Smad2, and Smad3 expression in lung tissue. ACE2 plasmid significantly decreased the expression of TGF-β1 and p-Smad2/3 but did not affect the expression of Smad2/Smad3 expression, indicating that ACE2 inhibited the TGF-β1/Smad2/Smad3 pathway in cells.

TGF-β1 Overexpression Abolished the Effects of ACE2 Plasmid on the EMT. To explore the involvement of TGF-β1 in the anti-EMT effects of ACE2, MLE-12 cells were treated with LPS and ACE2+TGF-β1 plasmid. Fig. 7A shows that the expression of TGF-β1 was significantly increased in the TGF-β1 plasmid group, indicating that the expression of TGF-β1 using the plasmid vector was successful. Fig. 7, B–D shows the expression of E-cadherin, α-SMA, and vimentin. E-cadherin expression was dramatically decreased in the model+ACE2+TGF-β1-plasmid group compared with model+ACE2-plasmid group. By contrast, α-SMA and vimentin expression was dramatically increased with the ACE2+TGF-β1-plasmid treatment. Taken together, these results indicated ACE2 inhibited the EMT in MLE-12 cells by downregulating TGF-β1.

Discussion

Although our understanding of ARDS has increased in recent years, the mortality rate of ARDS remains 35%–46%. Currently, the high mortality rate of patients with ARDS is

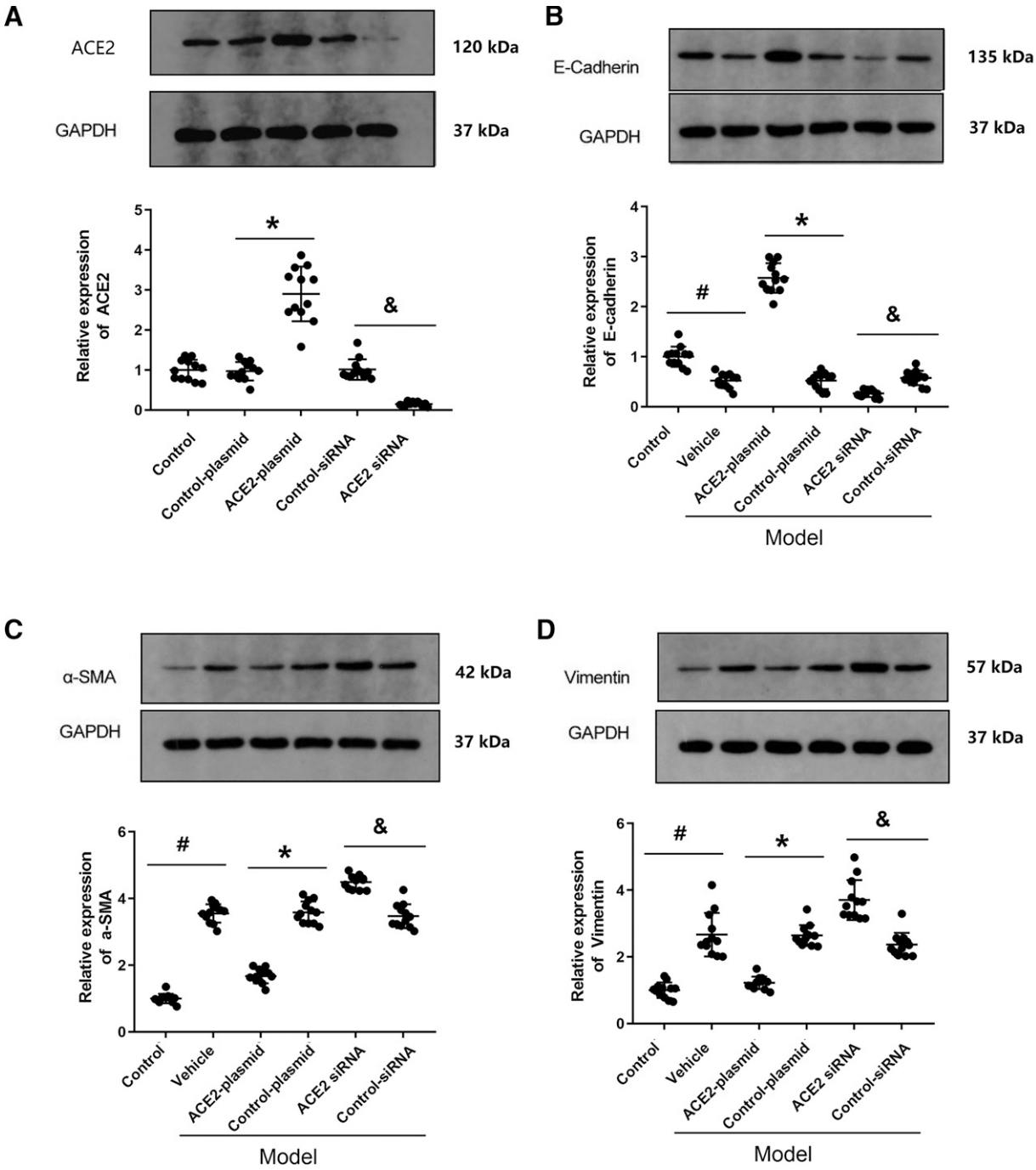

Fig. 5. The effects of ACE2 overexpression or siRNA on the EMT in MLE-12 cells. The mouse lung type II epithelial cell line MLE-12 was treated with LPS and ACE2 plasmid or ACE2 siRNA. Then, expression of E-cadherin, α-SMA, and vimentin was measured. (A) The representative images of western blot of ACE2 after cells were treated with ACE2 plasmid or ACE2 siRNA. (B–D) The representative images of western blot of E-cadherin, α-SMA, and vimentin and their relative changes. #, $P < 0.05$ compared with control; *, $P < 0.05$ compared with vehicle. $N = 12$. GAPDH, glyceraldehyde-3-phosphate dehydrogenase.

thought to be due to pulmonary fibrosis, which is also a key factor affecting the prognosis of ARDS (Zhang et al., 2015). In the acute inflammatory phase of ARDS, the cytotoxic mediators (including reactive oxygen species and nitrogen substances) released by infiltrating leukocytes and proteolytic enzymes lead to the injury (Zemans et al., 2009). Persistent injury and untimely injury repair are the main factors leading to a pathologic fibro proliferative reaction (Burnham et al., 2014). In some patients, macrophages, fibroblasts, and myofibroblasts persistently accumulate, resulting in excessive deposition of components of the ECM (Fahy et al., 2003), which is accompanied by the imbalance between profibrosis mediators and antifibrosis mediators and leads to fibroproliferative response (Fahy et al., 2003; White et al., 2008). In recent studies, epithelial cells were shown to be involved in the formation of renal fibrosis and liver fibrosis (Zhao et al., 2019; Zou et al., 2019). The damage and repair of lung epithelial cells also play a key role in pulmonary fibrosis (Zhang et al., 2015). If lung

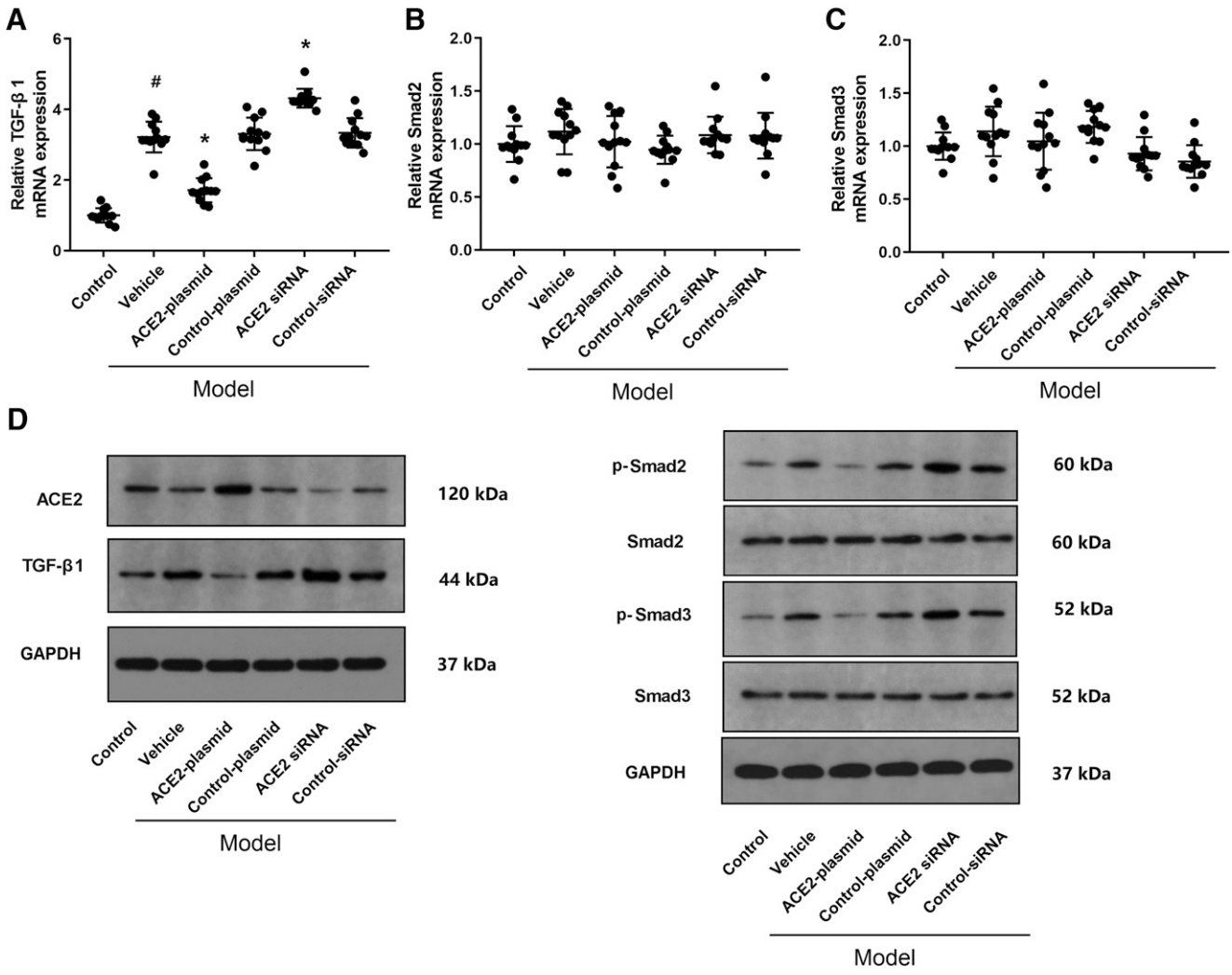

Fig. 6. Effects of ACE2 overexpression or siRNA on mRNA and protein levels of TGF-β1, Smad2, and Smad3 in MLE-12 cells. The MLE-12 cells were treated with ACE2 plasmid or ACE2 siRNA, and the mRNA and protein expression of TGF-β1, Smad2, and Smad3 in the lung were measured. (A–C) The mRNA levels of TGF-β1, Smad2, and Smad3 in cells. (D) The representative images of western blot. $^{\#}$, $P < 0.05$ compared with control; *, $P < 0.05$ compared with vehicle. $N = 12$.

epithelial cells are continuously damaged and excessively repaired, pulmonary fibrosis may occur (Quesnel et al., 2012). The present study results showed that LPS treatment could cause pulmonary fibrosis. H&E and Masson staining of lung tissue showed the integrity of lung structure was significantly damaged after LPS treatment (Fig. 1). The alveolar septum was thickened, and a large amount of blue-stained collagen was observed in the thickened area, indicating significant collagen deposition. The amount of collagen I and hydroxyproline in lung tissue as well as TGF-β1 levels in BALF were also significantly increased by LPS treatment (Fig. 2). These results suggested that LPS treatment successfully caused lung fibrosis.

Discovery of the ACE2 gene in recent years was a major breakthrough in the prevention and treatment of new targets of hypertension, diabetes, and other diseases (Liu et al., 2011). ACE2 can degrade Ang II to Ang1-7 and Ang I to Ang1-9, which can be further degraded to Ang1-7. Ang1-7 and its main receptor (MasR) constitute the ACE2/Ang1-7/MasR axis. Firstly, the results of the present study showed that ACE2 mRNA and protein expression in the mouse model of LPS-induced lung fibrosis were significantly decreased (Fig. 3), although the level of significance is not very high. The relative low level of significance may indicate that the ACE2 expression was regulated by multiple factors, which prevent the dramatic decrease of ACE2 in the LPS-induced lung fibrosis model. Secondly, the ACE2 activator DIZE attenuated LPS-caused lung fibrosis based on H&E and Masson staining and Ashcroft scores (Fig. 1). DIZE also significantly decreased the expression of α-SMA, collagen I, hydroxyproline, and TGF-β1 in the lung (Fig. 2), indicating that ACE2 can inhibit formation of collagen and activation of the TGF-β1 pathway, which is consistent with previous studies. Reportedly, ACE2 can slow down the pathologic progression of organ fibrosis by regulating the balance of angiotensin peptide and the production of inflammatory mediators and ECM and by inhibiting the process of oxidative stress. Consequently, ACE2 has become a novel target for intervention and prevention of organ fibrosis (Liu et al., 2011), which is also supported by our study.

TGF-β is a member of a group of cytokines with complex biologic functions (Chin et al., 2004). TGF-β1 is the main factor that promotes fibrosis in vivo as well as the proliferation and

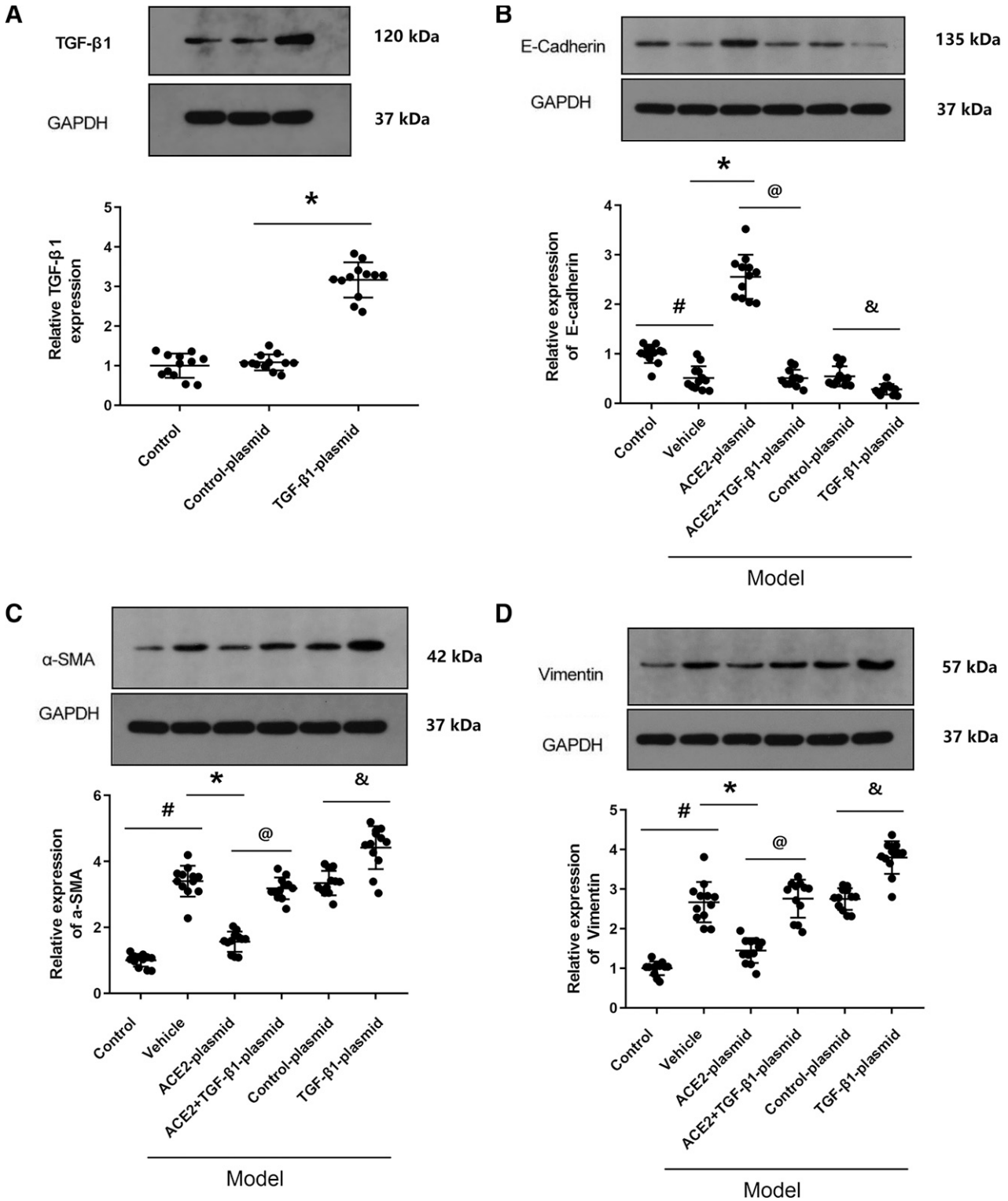

Fig. 7. Effects of TGF-β1 overexpression on the EMT in MLE-12 cells. MLE-12 cells were treated with LPS and ACE2+TGF-β1 plasmid, and expression of E-cadherin, α-SMA, and vimentin was measured. (A) The expression of TGF-β1 after cells were treated with TGF-β1 plasmid. (B–D) The representative images of western blot of E-cadherin, α-SMA, and vimentin and their relative changes. $^{\#}$, $P < 0.05$ compared with control; *, $P < 0.05$ compared with vehicle; $^{@}$, $P < 0.05$ compared with ACE2-plasmid; $^{\&}$, $P < 0.05$ compared with control-plasmid. $N = 12$. GAPDH, glyceraldehyde-3-phosphate dehydrogenase.

aggregation of fibroblasts; it also stimulates the growth of immature fibroblasts (Xu et al., 2003). TGF-β1 monoclonal antibody can partially inhibit the proliferation of fibroblasts and synthesis of collagen (Alsafadi et al., 2017). TGF-β1 can also promote the transformation of fibroblasts to myofibroblasts, an essential cell in the pathogenesis of pulmonary fibrosis (Giménez et al., 2017; Salgado et al., 2017). When pulmonary fibrosis occurs, TGF-β1 is distributed in macrophages,

eosinophils, alveolar type II epithelial cells, small bronchioles, bronchial epithelial cells, fibroblasts, and myofibroblasts in the lung (Sadar et al., 2016; Bamberg et al., 2018). Reportedly, TGF-β, Smad, mitogen-activated protein kinase, phosphatidylinositol 3-kinasec, and Jun N-terminal Kinase signaling pathways all participate in the occurrence of pulmonary fibrosis (Miyazawa et al., 2002; Tojo et al., 2005), in which the Smad signaling pathway is the classic pathway that mediates the signal transduction of TGF-β. The present study shows that the level of TGF-β1 in mice was increased (Fig. 3). The levels of Smad2 and Smad3 were unchanged, but the p-Smad2/Smad2 and p-Smad3/Smad3 ratios were significantly increased in the LPS group (Fig. 3). Thus, in the LPS-induced lung fibrosis mouse model, the TGF-β1/Smad2/Smad3 pathway was activated. Smad2 and Smad3 are TGF-β1 receptor substrates. In previous studies, upon bleomycin treatment, Smad3 in the cytoplasm continuously decreased, and its level in the nucleus transiently increased. Smad2/Smad3 phosphorylation and nuclear aggregation continuously increased, and Smad4 in the cytoplasm and nucleus transiently increased (Tatler et al., 2016). Smad3 deficiency can inhibit TGF-β1 overexpression and the progress of lung fibrosis. The regulation of Smad2/Smad3 protein expression was suggested to significantly participate in the advancement of pulmonary fibrosis. The mRNA and protein levels of TGF-β1 were both significantly inhibited by ACE2 inhibitor DIZE (Fig. 4). Although DIZE did not affect Smad2 and Smad3 mRNA and protein expression, it significantly inhibited the expression of TGF-β1 and the phosphorylation of Smad2/3 (Fig. 4), indicating that ACE2 suppressed the TGF-β1/Smad2/Smad3 pathway in vivo.

The EMT is closely associated with organ fibrosis (Puisieux et al., 2014). Characteristics of the EMT mainly include the disappearance of tight junctions between cells, loss of normal polarity, deformed and remolded cytoskeleton, and increased α-SMA expression (Dos Santos, 2008; Nieto et al., 2016). Therefore, to examine the possible role of ACE2 on LPS-induced lung fibrosis, MLE-12 cells were treated with LPS and ACE2 overexpression or siRNA before the EMT changes were measured. LPS significantly reduced E-cadherin level and increased α-SMA and vimentin expression in MLE-12 cells (Fig. 5), indicating LPS treatment could induce EMT in MLE-12 cells. ACE2 overexpression increased E-cadherin expression but decreased α-SMA and vimentin expression (Fig. 5); siRNA treatment of ACE2 resulted in opposite changes (Fig. 5), indicating ACE2 inhibited the EMT. These results indicated the EMT of lung type II epithelial cells may contribute to LPS-induced lung fibrosis, which can be reversed by ACE2.

To further confirm the role of the TGF-β1/Smad2/Smad3 pathway, cells were treated with ACE2 plasmid or ACE2 siRNA before the TGF-β1, Smad2, and Smad3 mRNA and protein expression were measured. Similar to the in vivo study, the TGF-β1 levels were both significantly reduced by ACE2 plasmid but increased by ACE2 siRNA (Fig. 6). ACE2 plasmid significantly decreased the p-Smad2/3 levels, indicating that ACE2 suppressed the TGF-β1/Smad2/Smad3 pathway (Fig. 6). We have conducted a series of experiments to explore the effect of ACE2 on the expression of TGF-β1. The results of Fig. 2E; Fig. 4, A and D; and Fig. 6, A and D indicated that ACE2 downregulate TGF-β1 in the lung tissue of mice but didn't indicate the anti-EMT effect of ACE2 is dependent on TGF-β1. Therefore, we conducted the experiments of Fig. 7 to see whether ACE2 inhibited EMT via TGF-β1. We used the TGF-β1 overexpressing plasmid vector to restore the expression of TGF-β1, then observed the expression of EMT-related proteins (E-cadherin, α-SMA, and vimentin). The results showed that overexpression of TGF-β1 abolished the effect of ACE2 overexpressing plasmid vector on the expression of these proteins, indicating that the anti-EMT effect of ACE2 is dependent on TGF-β1. Combined with the previous experiments (Fig. 2E; Fig. 4, A and D; and Fig. 6, A and D), we can conclude that ACE2 inhibited EMT by downregulating TGF-β1. Combined with the in vivo study, it was indicated that ACE2 can inhibit the TGF-β1/Smad2/Smad3 pathway in lung type II epithelial cells, thus reversing their EMT and lung fibrosis.

In conclusion, the present study provides basic research data for the application of ACE2 in the lung fibrosis and clarifies the intervention mechanism of ACE2 in pulmonary fibrosis, which may be clinically relevant. The results also improve our understanding of TGF-β1/Smad2/Smad3 signaling in lung fibrosis. The regulatory mechanism is of theoretical significance for determining the molecular mechanism of pulmonary fibrosis induced by ALI.

Authorship Contributions

Participated in research design: X. Lin, Gao.
Conducted experiments: W. Lin.
Contributed new reagents or analytic tools: Zhuang.
Performed data analysis: Zhuang.
Wrote or contributed to the writing of the manuscript: X. Lin., Gao.

References

Alsafadi HN, Staab-Weijnitz CA, Lehmann M, Lindner M, Peschel B, Königshoff M, and Wagner DE (2017) An ex vivo model to induce early fibrosis-like changes in human precision-cut lung slices. *Am J Physiol Lung Cell Mol Physiol* **312**:L896–L902.

Antunes MA, Laffey JG, Pelosi P, and Rocco PR (2014) Mesenchymal stem cell trials for pulmonary diseases. *J Cell Biochem* **115**:1023–1032.

Attisano L and Wrana JL (2002) Signal transduction by the TGF-beta superfamily. *Science* **296**:1646–1647.

Bamberg A, Redente EF, Groshong SD, Tuder RM, Cool CD, Keith RC, Edelman BL, Black BP, Cosgrove GP, Wynes MW, et al. (2018) Protein Tyrosine Phosphatase-N13 Promotes Myofibroblast Resistance to Apoptosis in Idiopathic Pulmonary Fibrosis. *Am J Respir Crit Care Med* **198**:914–927.

Burnham EL, Janssen WJ, Riches DW, Moss M, and Downey GP (2014) The fibroproliferative response in acute respiratory distress syndrome: mechanisms and clinical significance. *Eur Respir J* **43**:276–285.

Butt Y, Kurdowska A, and Allen TC (2016) Acute Lung Injury: A Clinical and Molecular Review. *Arch Pathol Lab Med* **140**:345–350.

Chin D, Boyle GM, Parsons PG, and Coman WB (2004) What is transforming growth factor-beta (TGF-beta)? *Br J Plast Surg* **57**:215–221.

Dos Santos CC (2008) Advances in mechanisms of repair and remodelling in acute lung injury. *Intensive Care Med* **34**:619–630.

Fahy RJ, Lichtenberger F, McKeegan CB, Nuovo GJ, Marsh CB, and Wewers MD (2003) The acute respiratory distress syndrome: a role for transforming growth factor-beta 1. *Am J Respir Cell Mol Biol* **28**:499–503.

Fang Y, Gao F, and Liu Z (2019) Angiotensin-converting enzyme 2 attenuates inflammatory response and oxidative stress in hyperoxic lung injury by regulating NF-κB and Nrf2 pathways. *QJM* **112**:914–924.

George PM, Wells AU, and Jenkins RG (2020) Pulmonary fibrosis and COVID-19: the potential role for antifibrotic therapy. *Lancet Respir Med* **8**:807–815.

Giménez A, Duch P, Puig M, Gabasa M, Xaubet A, and Alcaraz J (2017) Dysregulated Collagen Homeostasis by Matrix Stiffening and TGF-β1 in Fibroblasts from Idiopathic Pulmonary Fibrosis Patients: Role of FAK/Akt. *Int J Mol Sci* **18**:2431.

Huang H, Wang J, Liu Z, and Gao F (2020) The angiotensin-converting enzyme 2/angiotensin (1-7)/mas axis protects against pyroptosis in LPS-induced lung injury by inhibiting NLRP3 activation. *Arch Biochem Biophys* **693**:108562.

Kobori H, Nangaku M, Navar LG, and Nishiyama A (2007) The intrarenal renin-angiotensin system: from physiology to the pathobiology of hypertension and kidney disease. *Pharmacol Rev* **59**:251–287.

Li G, Xu YL, Ling F, Liu AJ, Wang D, Wang Q, and Liu YL (2012) Angiotensin-converting enzyme 2 activation protects against pulmonary arterial hypertension through improving early endothelial function and mediating cytokines levels. *Chin Med J (Engl)* **125**:1381–1388.

Li Y, Li H, Liu S, Pan P, Su X, Tan H, Wu D, Zhang L, Song C, Dai M, et al. (2018) Pirfenidone ameliorates lipopolysaccharide-induced pulmonary inflammation and fibrosis by blocking NLRP3 inflammasome activation. *Mol Immunol* **99**:134–144.

Liu CX, Hu Q, Wang Y, Zhang W, Ma ZY, Feng JB, Wang R, Wang XP, Dong B, Gao F, et al. (2011) Angiotensin-converting enzyme (ACE) 2 overexpression ameliorates

glomerular injury in a rat model of diabetic nephropathy: a comparison with ACE inhibition. *Mol Med* **17**:59–69.
Liu Y (2006) Renal fibrosis: new insights into the pathogenesis and therapeutics. *Kidney Int* **69**:213–217.
Lu Q, Harrington EO, Jackson H, Morin N, Shannon C, and Rounds S (1985) Transforming growth factor-beta1-induced endothelial barrier dysfunction involves Smad2-dependent p38 activation and subsequent RhoA activation. *J Appl Physiol* **101**:375–384.
McDonald LT (2021) Healing after COVID-19: are survivors at risk for pulmonary fibrosis? *Am J Physiol Lung Cell Mol Physiol* **320**:L257–L265.
Mackinnon AC, Gibbons MA, Farnworth SL, Leffler H, Nilsson UJ, Delaine T, Simpson AJ, Forbes SJ, Hirani N, Gauldie J, et al. (2012) Regulation of transforming growth factor-β1-driven lung fibrosis by galectin-3. *Am J Respir Crit Care Med* **185**:537–546.
Miyazawa K, Shinozaki M, Hara T, Furuya T, and Miyazono K (2002) Two major Smad pathways in TGF-beta superfamily signalling. *Genes Cells* **7**:1191–1204.
Nieto MA, Huang RY, Jackson RA, and Thiery JP (2016) Emt: 2016. *Cell* **166**:21–45.
Puisieux A, Brabletz T, and Caramel J (2014) Oncogenic roles of EMT-inducing transcription factors. *Nat Cell Biol* **16**:488–494.
Qaradakhi T, Gadanec LK, McSweeney KR, Tacey A, Apostolopoulos V, Levinger I, Rimarova K, Egom EE, Rodrigo L, Kruzliak P, et al. (2020) The potential actions of angiotensin-converting enzyme II (ACE2) activator diminazene aceturate (DIZE) in various diseases. *Clin Exp Pharmacol Physiol* **47**:751–758.
Quesnel C, Piednoir P, Gelly J, Nardelli L, Garnier M, Leçon V, Lasocki S, Bouadma L, Philip I, Elbim C, et al. (2012) Alveolar fibrocyte percentage is an independent predictor of poor outcome in patients with acute lung injury. *Crit Care Med* **40**:21–28.
Sadar S, Kaspate D, and Vyawahare N (2016) Protective effect of L-glutamine against diabetes-induced nephropathy in experimental animal: Role of KIM-1, NGAL, TGF-β1, and collagen-1. *Ren Fail* **38**:1483–1495.
Salgado RM, Cruz-Castañeda O, Elizondo-Vázquez F, Pat L, De la Garza A, Cano-Colín S, Baena-Ocampo L, and Krötzsch E (2017) Maltodextrin/ascorbic acid stimulates wound closure by increasing collagen turnover and TGF-β1 expression in vitro and changing the stage of inflammation from chronic to acute in vivo. *J Tissue Viability* **26**:131–137.
Santos RA, Simoes e Silva AC, Maric C, Silva DM, Machado RP, de Buhr I, Heringer-Walther S, Pinheiro SV, Lopes MT, Bader M, et al. (2003) Angiotensin-(1-7) is an endogenous ligand for the G protein-coupled receptor Mas. *Proc Natl Acad Sci USA* **100**:8258–8263.
Shi H, Han X, Jiang N, Cao Y, Alwalid O, Gu J, Fan Y, and Zheng C (2020) Radiological findings from 81 patients with COVID-19 pneumonia in Wuhan, China: a descriptive study. *Lancet Infect Dis* **20**:425–434.
Shu J, He X, Zhang L, Li H, Wang P and Huang X (2015) Human amnion mesenchymal cells inhibit lipopolysaccharide-induced TNF-α and IL-1β production in THP-1 cells. *Biol Res* **48**:15–62.
Simko F, Hrenak J, Adamcova M, and Paulis L (2021) Renin-Angiotensin-Aldosterone System: Friend or Foe-The Matter of Balance. Insight on History, Therapeutic Implications and COVID-19 Interactions. *Int J Mol Sci* **22**:3217.
Tale S, Ghosh S, Meitei SP, Kolli M, Garbhapu AK, and Pudi S (2020) Post-COVID-19 pneumonia pulmonary fibrosis. *QJM* **113**:837–838.
Tao L, Qiu Y, Fu X, Lin R, Lei C, Wang J, and Lei B (2016) Angiotensin-converting enzyme 2 activator diminazene aceturate prevents lipopolysaccharide-induced inflammation by inhibiting MAPK and NF-κB pathways in human retinal pigment epithelium. *J Neuroinflammation* **13**:35.
Tatler AL, Goodwin AT, Gbolahan O, Saini G, Porte J, John AE, Clifford RL, Violette SM, Weinreb PH, Parfrey H, et al. (2016) Amplification of TGFβ Induced ITGB6 Gene Transcription May Promote Pulmonary Fibrosis. *PLoS One* **11**:e0158047.
Tojo M, Hamashima Y, Hanyu A, Kajimoto T, Saitoh M, Miyazono K, Node M, and Imamura T (2005) The ALK-5 inhibitor A-83-01 inhibits Smad signaling and epithelial-to-mesenchymal transition by transforming growth factor-beta. *Cancer Sci* **96**:791–800.
Wan H, Xie T, Xu Q, Hu X, Xing S, Yang H, Gao Y, and He Z (2019) Thy-1 depletion and integrin β3 upregulation-mediated PI3K-Akt-mTOR pathway activation inhibits lung fibroblast autophagy in lipopolysaccharide-induced pulmonary fibrosis. *Lab Invest* **99**:1636–1649.
Wang L, Yuan R, Yao C, Wu Q, Christelle M, Xie W, Zhang X, Sun W, Wang H, and Yao S (2014) Effects of resolvin D1 on inflammatory responses and oxidative stress of lipopolysaccharide-induced acute lung injury in mice. *Chin Med J (Engl)* **127**:803–809.
White AJ, Cheruvu SC, Sarris M, Liyanage SS, Lumbers E, Chui J, Wakefield D, and McCluskey PJ (2015) Expression of classical components of the renin-angiotensin system in the human eye. *J Renin Angiotensin Aldosterone Syst* **16**:59–66.
White KE, Ding Q, Moore BB, Peters-Golden M, Ware LB, Matthay MA, and Olman MA (2008) Prostaglandin E2 mediates IL-1beta-related fibroblast mitogenic effects in acute lung injury through differential utilization of prostanoid receptors. *J Immunol* **180**:637–646.
Wu CS, Wu PH, Fang AH, and Lan CC (2012) FK506 inhibits the enhancing effects of transforming growth factor (TGF)-β1 on collagen expression and TGF-β/Smad signalling in keloid fibroblasts: implication for new therapeutic approach. *Br J Dermatol* **167**:532–541.
Xu YD, Hua J, Mui A, O'Connor R, Grotendorst G, and Khalil N (2003) Release of biologically active TGF-beta1 by alveolar epithelial cells results in pulmonary fibrosis. *Am J Physiol Lung Cell Mol Physiol* **285**:L527–L539.
Zemans RL, Colgan SP, and Downey GP (2009) Transepithelial migration of neutrophils: mechanisms and implications for acute lung injury. *Am J Respir Cell Mol Biol* **40**:519–535.
Zhang H and Sun GY (2005) LPS induces permeability injury in lung microvascular endothelium via AT(1) receptor. *Arch Biochem Biophys* **441**:75–83.
Zhang L, Wang J, Liang J, Feng D, Deng F, Yang Y, Lu Y, and Hu Z (2018) Propofol prevents human umbilical vein endothelial cell injury from Ang II-induced apoptosis by activating the ACE2-(1-7)-Mas axis and eNOS phosphorylation. *PLoS One* **13**:e0199373.
Zhang R, Pan Y, Fanelli V, Wu S, Luo AA, Islam D, Han B, Mao P, Ghazarian M, Zeng W, et al. (2015) Mechanical Stress and the Induction of Lung Fibrosis via the Midkine Signaling Pathway. *Am J Respir Crit Care Med* **192**:315–323.
Zhang X, Zheng J, Yan Y, Ruan Z, Su Y, Wang J, Huang H, Zhang Y, Wang W, Gao J, et al. (2019) Angiotensin-converting enzyme 2 regulates autophagy in acute lung injury through AMPK/mTOR signaling. *Arch Biochem Biophys* **672**:108061.
Zhao S, Jiang JT, Li D, Zhu YP, Xia SJ, and Han BM (2019) Maternal exposure to di-n-butyl phthalate promotes Snail1-mediated epithelial-mesenchymal transition of renal tubular epithelial cells via upregulation of TGF-β1 during renal fibrosis in rat offspring. *Ecotoxicol Environ Saf* **169**:266–272.
Zou Y, Li S, Li Z, Song D, Zhang S, and Yao Q (2019) MiR-146a attenuates liver fibrosis by inhibiting transforming growth factor-β1 mediated epithelial-mesenchymal transition in hepatocytes. *Cell Signal* **58**:1–8.

Address correspondence to: Xingsheng Lin, Department of Intensive Care Unit, Shengli Clinical Medical College of Fujian Medical University, Fujian Provincial Hospital, 134 East Street, Fuzhou, Fujian 350001, China. E-mail: xingshengicu@outlook.com; or Fengying Gao, Department of Respiratory Medicine, Shanghai Construction Group Hospital, Shanghai 200083, China. E-mail: fengyinggao@outlook.com